

ENC-2022-0354

DEVELOPMENT AND APPLICATION OF A WIDE-BAND APPROACH BASED ON THE WEIGHTED-SUM-OF-GRAY-GASES MODEL FOR PROBLEMS WITH NON-GRAY WALLS

Roberta Juliana Collet da Fonseca

Francis Henrique Ramos França

Department of Mechanical Engineering, Federal University of Rio Grande do Sul, Porto Alegre, Brazil

roberta.fonseca@ufrgs.br

frfranca@mecanica.ufrgs.br

Guilherme Crivelli Fraga

Clean Energy Engineering Center, University of Connecticut, Storrs, United States of America

guilherme.fraga@uconn.edu

Abstract. *The spectral modeling of the radiative properties of participating gases is one of the most significant research fields in the heat transfer by thermal radiation. However, the correct representation of the spectral dependence of the absorption coefficient of a participating gas, such as water vapor and carbon dioxide, is a difficult undertaking, since it depends on the solution of the line-by-line (LBL) integration to accurately solve the radiative transfer equation (RTE). When the medium is contained within a non-gray enclosure and the spectral dependence of the boundaries must also be taken into account, this complexity increases even further. In this framework, to compute the radiative exchanges between a participating medium and non-gray walls, the present paper proposes the development and application of a wide-band model based on the weighted-sum-of-gray-gases (WSGG). In this method, the spectrum is divided into a set of regions and these spectral intervals are synchronized with the spectral emissivity distribution of the non-gray boundaries. The WSGG model is used to solve the contribution of the radiative heat flux and radiative heat source of each one of these segments. The results show that the proposed methodology led to maximum deviations of 8% compared to the LBL solution.*

Keywords: *thermal radiation, non-gray walls, spectral intervals, wide-band models*

1. INTRODUCTION

The radiative heat transfer is important in many physical and engineering processes. Due to the presence of participating gases, soot and particulates at elevated temperatures, such as furnaces for heat treatment, steam generators, engine chambers and flares in the oil industry, the thermal radiation is typically the dominant mechanism of heat transfer in the combustion systems (Modest, 2013; Modest and Haworth, 2016). The calculation of the thermal radiation in participating gases, such as water vapor and carbon dioxide, is a considerably complex task in virtue of the strongly irregular dependence on the wavenumber of the radiative properties of these chemical species. Furthermore, the flames are characterized by intense variations in their temperature and concentration fields of the participating species (Modest, 2013).

In the most engineering applications, the emission and absorption of the thermal radiation in gases result from transitions in vibrational and rotational energy states, generating spectral lines distributed around specific wavenumbers (Howell *et al.*, 2016). Currently, databases related to spectral lines are available, such as HITEMP (Rothman *et al.*, 2010) and HITRAN (Gordon *et al.*, 2021), from which it is possible to obtain the properties of the gases with a high level of detailing. The thermal radiation can be calculated with considerable accuracy through line-by-line (LBL) integration (Taine, 1983), summing the contributions of the emission and absorption of each one of the spectral lines. However, this methodology requires a prohibitive computational cost in some scenarios, due to the large number of lines that cover the radiation spectrum. The absorption spectrum of a gas can contain hundreds of thousands or millions of spectral lines. In the modeling of real engineering problems, such as in combustion processes, which may involve irregular geometries and the coupling of multiple phenomena, for instance, chemical kinetics, turbulent transport and heat transfer combining convection and radiation, the computation of each spectral line of the spectrum is a practically unfeasible task, thus establishing the need to develop reliable models of spectral integration.

In this framework, the development and application of gas models represent a useful alternative to reduce the computational cost in the solution of the spectral part of the radiative transfer problem without incurring in a loss of the accuracy of the results. In the radiation field, the literature continues to present studies from the simplest models, such as the gray gas (GG) and the weighted-sum-of-gray-gases (WSGG) (Hottel and Sarofim, 1967), to the more recent models based on the distribution functions built directly from the spectrum, such as the spectral line-based WSGG (SLW) model (Denison and Webb, 1993), the full-spectrum correlated- k (FSK) distribution (Modest and Zhang, 2000) and the cumulative wavenumber (CW) method (Solovjov and Webb, 2002). The WSGG model, though older, has recently experienced ongoing improvements, leading to conclusions that are equally as accurate as the most sophisticated spectral models, which has led to its use in recent papers (Dorigon *et al.*, 2013; Cassol *et al.*, 2014; Coelho and França, 2018; Wang and Xuan, 2019; Bordbar *et al.*, 2021; He *et al.*, 2021; Silva *et al.*, 2021; Selhorst *et al.*, 2022).

The boundaries of the domain are frequently portrayed as black surfaces in the literature on the use of gas models. This assumption enables the decoupling of the spectral integration of the medium in relation to the surface, in order to develop spectral gas models regardless of the conditions at the boundaries. In contrast to research that works on the assumption that boundaries are black, the study of radiation exchanges between participating gases and non-gray surfaces has received little attention in the literature. At the non-gray boundaries, the radiative transfer equation (RTE) must be solved iteratively, in order to account for the reflection of the radiation intensity on the walls, which is given as a function of the intensity incident on them (which, in turn, depends on the properties of the medium). This fact makes the calculation computationally more expensive than on black surfaces, in which the intensities at the boundaries are known and, therefore, the RTE is solved in a single step. Some examples of studies about this topic are found in Denison and Webb, 1994, Solovjov *et al.*, 2013, Fonseca *et al.*, 2018, Bordbar *et al.*, 2019, Liu *et al.*, 2019, and Fonseca *et al.*, 2021b.

In the present paper, the wide-band based on WSGG (WBW) model is applied to solve the spectral integration of the RTE. This model aims to refine the spectrum, dividing it into a series of spectral intervals, and using it to solve each one of these intervals, in order to improve the standard WSGG model. A preliminary implementation of this method was recently presented by Fonseca *et al.*, 2021a, but with a participating medium composed only of pure H₂O, and not a mixture of water vapor and carbon dioxide, as it will be explored in this work and it was studied in detail in Fonseca, 2022. In this approach, the one-dimensional system presents non-gray boundaries, i.e., the walls have radiative properties (spectral emissivity and absorptivity) that depend on the wavenumber. The spectrum was divided into five spectral intervals and to each one of them was assigned 4 gray gases employing the WBW correlations generated by Fonseca, 2022, for a gaseous mixture composed of H₂O and CO₂ in the mole fraction ratio of 2. The regions into which the spectrum was divided and the spectral ranges of the emissivity profile of the surfaces were assumed to be coincident. The results obtained with the WBW model are compared against the LBL solution, whose the absorption spectra were generated through the HITEMP 2010 database for a wavenumber range of $0 \text{ cm}^{-1} < \eta < 25 \text{ 000 cm}^{-1}$, with a spectral resolution of 0.067 cm^{-1} .

2. RADIATION MODELING

This section presents a discussion of the concepts about thermal radiation, the governing equations and the theoretical basis on which the proposed model was developed.

2.1 The line-by-line method

For a participating medium without scattering, the variation of the spectral intensity is governed by the RTE, such as (Modest, 2013; Howell *et al.*, 2016)

$$\frac{dI_\eta}{ds} = -\kappa_\eta I_\eta + \kappa_\eta I_{b\eta}, \quad (1)$$

where I_η is the spectral radiation intensity, κ_η is the spectral absorption coefficient of the medium and $I_{b\eta}$ is the blackbody spectral radiation intensity. This last quantity is computed from the Planck's distribution function for a wavenumber η and a temperature T along a given path.

For a diffuse and non-gray surface located at $x = 0$, the RTE is subjected to the following boundary condition:

$$I_\eta \Big|_{x=0} = I_{\eta,0} = \varepsilon_\eta I_{b\eta,0} + (1 - \alpha_\eta) \overline{I_{\eta,i}}, \quad (2)$$

in which ε_η and α_η are the spectral emissivity and the spectral absorptivity of the surface, respectively, $I_{b\eta,0}$ is the spectral blackbody intensity evaluated at the boundary $x = 0$ and $\overline{I_{\eta,i}}$ is the average spectral intensity that is incident on the wall. For the other wall, i.e., $x = L$, the boundary condition is analogous to the above equation; however, it is evaluated on the right boundary. The quantity $\overline{I_{\eta,i}}$ is defined as

$$\overline{I_{\eta,i}} = \frac{1}{\pi} \int_0^{2\pi} I_{\eta,i} \cos(\theta_i) d\omega_i, \quad (3)$$

where $I_{\eta,i}$ is the spectral intensity reaching on the wall surface from direction $d\omega_i$. On the right side of Eq. (2), the first and second terms account for the emission and reflection from the boundary, respectively. In problems in which the walls are perfectly diffuse, $\varepsilon_\eta = \alpha_\eta$.

Once Eq. (1) subjected to Eq. (2) is solved, the total radiative intensity can be determined as $I = \int_0^\infty I_\eta d\eta$. In an analogous way, the total emissivity and absorptivity of the wall are defined by integrating the spectral intensity that leaves the boundary over the entire spectrum, such as $I_0 = \int_0^\infty I_{\eta,0} d\eta$. Integrating the above equation yields

$$I_0 = \varepsilon I_{b,0} + (1 - \alpha) \bar{I}_i, \quad (4)$$

in which the blackbody radiative intensity evaluated on the left wall (i.e., at $x = 0$) is given by

$$I_{b,0} = \int_0^\infty I_{b\eta,0} d\eta, \quad (5)$$

and the incident intensity is calculated as

$$\bar{I}_i = \int_0^\infty \bar{I}_{\eta,i} d\eta. \quad (6)$$

Finally, the the total emissivity ε and the total absorptivity α of the surface are given, respectively, by

$$\varepsilon = \frac{\int_0^\infty \varepsilon_\eta I_{b\eta,0} d\eta}{I_{b,0}}, \quad (7)$$

$$\alpha = \frac{\int_0^\infty \alpha_\eta \bar{I}_{\eta,i} d\eta}{\bar{I}_i}, \quad (8)$$

After solving the spectral intensity of each wavenumber η according to Eq. (1) via Eq. (3), the total intensity I can be calculated simply integrating I_η over the whole spectrum. Therefore, the calculation of the variation regarding the wavenumber of the spectral emissivity and absorptivity is inherent to the LBL method, which means that the solution of the spectral intensity for each value of η is not a difficult task, even though it is a procedure in which an elevated computational time is required. Nevertheless, for gas spectral models, in which the spectral absorption coefficient is commonly modeled along the spectrum without regard to specific spectral locations, it becomes more convenient to define constant values for the wall emissivity ε and absorptivity α for these cases.

Finally, integrating the RTE and solving for the spectral radiation intensities for a set of directions, it is also possible to determine the radiative heat flux and radiative heat source at each position in the domain, such that

$$q_r(x) = \sum_{l=1}^{n_d} \int_\eta 2\pi\mu_l\omega_l \left[I_{\eta,l}^+(x) - I_{\eta,l}^-(x) \right] d\eta, \quad (9)$$

$$S_r(x) = \sum_{l=1}^{n_d} \int_\eta 2\pi\kappa_\eta\omega_l \left[I_{\eta,l}^+(x) + I_{\eta,l}^-(x) \right] - 4\pi\kappa_\eta I_{b\eta}(x) d\eta, \quad (10)$$

where n_d is the number of directions used for the directional integration of the RTE, μ_l is the directional cosine and ω_l is the weight for the Gauss-Legendre quadrature; the terms $I_{\eta,l}^+$ and $I_{\eta,l}^-$ are the positive and negative spectral radiation intensities, respectively.

2.2 Application to global spectral models

The methodology discussed in this section to exemplify the application of the proposed model for non-gray surfaces to gas models will be presented in the context of the WBW model, which is derived from the standard WSGG model. Details on the standard formulation of the WSGG model can be found in Hottel and Sarofim, 1967, Modest, 2013, and Howell *et al.*, 2016.

As discussed in the present study, the solution of the RTE requires a spectral integration over the entire spectrum. Despite offering an accurate solution for the problem, the LBL method has a high computational cost, what makes it impractical for use in real situations. Therefore, it becomes more important to develop and apply global spectral models, such as the WSGG model, which simplify the treatment of the behavior of the absorption coefficient of a gas in these cases. In this model, the irregular behavior of the absorption coefficient of a gas is replaced by a small set of gray gases, with uniform absorption coefficients, plus the transparent windows. The gray gases are assumed to be randomly spread along the spectrum. The pressure-absorption coefficient of each gray gas occupies a non-contiguous portion of the spectrum and is

assumed to be independent of temperature and wavenumber. The effect of the mole fraction of the participating species is described in the method through its partial pressure p_a .

The wide-band model based on WSGG (WBW) (Fonseca *et al.*, 2021a; Fonseca, 2022) is an attempt to enhance the WSGG model by the development of a technique that involves segmenting the radiation spectrum into a set of spectral intervals. For each spectral interval, a set of gray gases is assigned and the WSGG model is used to solve the contributions of the RTE, the radiative heat flux and the radiative heat source. The global results are given by a summation of the contributions from each one of these regions. The advantage of the proposed method is that, although it is a spectral model in which it is not possible to define the location of the gray gases, as the spectrum was divided into intervals, even if it is not possible to specify where the gases are, it is known that their positions are restricted to the spectral bands. In this way, the coupling of the radiative properties of gases with those of non-gray surfaces becomes simpler.

In this study, a methodology to compute the radiative exchanges between a participating medium and non-gray walls is proposed. Nevertheless, the coupling between the spectral treatment of the radiative properties of the medium and surfaces is an issue in the development of a model for this purpose. In these scenarios, it is impossible to directly relate the solution of the RTE through a global model with non-gray surfaces, since the information about the spectral position of the gray gases is lost. On the other hand, since the variation of the absorption coefficient of the gases in band models is known, the coupling can be carried out immediately. In the present study, it was assumed that the regions into which the spectrum was divided coincide with the intervals of the spectral distribution of the emissivities of the surfaces, which are considered identical, for simplicity. In future works, it is planned to find other more real ways of coupling the spectral intervals of the WBW model with the emissivity profiles of the non-gray boundaries.

Adopting the hypotheses of the WBW model for an arbitrary spectral interval k and a gray gas j , the RTE has the format below

$$\frac{dI_{j,k}}{dx} = -\kappa_{pj,k} p_a I_{j,k} + \kappa_{pj,k} p_a a_{j,k} f_k I_b, \quad (11)$$

In the above equation, $\kappa_{pj,k}$ is the pressure-absorption coefficient of the gray gas j , $I_{j,k}$ is the partial intensity of the gray gas j , $a_{j,k}$ is the temperature coefficient of the gas j , f_k is the fraction of blackbody energy that emanates from the spectral interval $\Delta\eta_k$, all of them in relation to the spectral band k , and I_b is the total blackbody radiation intensity. The parameters $\kappa_{pj,k}$ and $a_{j,k}$ of the k -th band can be determined from fittings of LBL data of emittance through the high-resolution spectral databases, such as HITEMP 2010. The emittance ϵ for each spectral interval $\Delta\eta_k$ is computed as

$$\epsilon_k = \frac{\pi \int_{\Delta\eta_k} I_{b\eta} [1 - \exp(-\kappa_{p\eta} p_a S)] d\eta}{\int_{\Delta\eta_k} I_{b\eta} d\eta}, \quad (12)$$

in which the denominator of the above equation is given by $\int_{\Delta\eta_k} I_{b\eta} d\eta = f_k I_b$, S is the path length and $\kappa_{p\eta} = \kappa_{\eta}/p_a$ is the spectral pressure-absorption coefficient.

Under the assumptions of the WBW model, Eq. (12) becomes

$$\epsilon_k = \sum_{j=1}^J a_j(T) [1 - \exp(-\kappa_{pj} p_a S)]. \quad (13)$$

Integrating Eq. (11) over the interval $\Delta\eta_k$ and assuming an arbitrary band k , it is subjected to the following boundary condition

$$I_{j,k} \Big|_{x=0} = I_{j,k,0} = \int_{\Delta\eta_k} [\varepsilon_{\eta,k} I_{b\eta,0} + (1 - \alpha_{\eta,k}) \overline{I_{\eta,i,k}}] d\eta = \varepsilon_k a_{j,k,0} f_{k,0} I_{b,0} + (1 - \alpha_k) \overline{I_{j,i,k}}, \quad (14)$$

where ε_k and α_k are the partial emissivity and absorptivity, both in relation to the boundary; the term $f_{k,0}$ is multiplying the blackbody total intensity I_b , because is necessary to measure the energy fraction of blackbody that is emitted in each spectral interval. For a spectral interval k , the emissivity and absorptivity are given, respectively, by

$$\varepsilon_k = \frac{\int_{\Delta\eta_k} \varepsilon_{\eta,k} I_{b\eta,0} d\eta}{a_{j,0} I_{b,0}}, \quad (15)$$

$$\alpha_k = \frac{\int_{\Delta\eta_k} \alpha_{\eta,k} \overline{I_{\eta,i,k}} d\eta}{\overline{I_i}}. \quad (16)$$

For the calculation of the radiative heat flux and radiative heat source also is required to account for the fraction f_k of

each segment in which the spectrum was divided. So, q_r and S_r are computed as

$$q_r(x) = \sum_{k=1}^{n_b} \sum_{l=1}^{n_d} \sum_{j=1}^J 2\pi\mu_l\omega_l \left[I_{j,l,k}^+(x) - I_{j,l,k}^-(x) \right], \quad (17)$$

$$S_r(x) = \sum_{k=1}^{n_b} \sum_{l=1}^{n_d} \sum_{j=1}^J 2\pi\kappa_{p,j,k} p_a \omega_l \left[I_{j,l,k}^+(x) + I_{j,l,k}^-(x) \right] - 4\pi\kappa_{p,j,k} p_a a_{j,k} f_k I_b(x), \quad (18)$$

in which n_b is the number of segments in which the spectrum was divided, and $I_{j,l,k}^+$ and $I_{j,l,k}^-$ are the radiation intensities of the gray gas j in the positive and negative directions.

2.3 The problem under study

In this paper, the heat transfer by thermal radiation for a one-dimensional medium slab was investigated. The 1D domain is composed by two diffuse, non-gray walls that bound a participating medium, which is formed by a non-homogeneous and non-isothermal mixture of water vapor and carbon dioxide. The temperature and mole fraction profiles evaluated are described in Section 3. The distance between the plates is $L = 1$ m and the total pressure is $p = 1$ atm. The domain under study is shown in Fig. 1. The WBW model, which was preliminarily presented in Fonseca *et al.*, 2021a, was used to solve the spectral integration of the RTE and the directional integration was carried out with the discrete ordinates method (DOM) for 12 directions, following the criteria proposed by Lathrop and Carlson, 1964. The spatial domain is divided into 200 equal-sized cells. The choice and adoption of these parameters of directional and spatial discretizations were discussed in detail in Fonseca, 2022, and it was proved to be adequate for simulations with the same physical conditions studied in this work.

The spectral emissivity distribution for the non-gray walls is given by a five-band stepwise variation, such that: $\varepsilon_\eta = 0.5$ for $0 \text{ cm}^{-1} < \eta < 1000 \text{ cm}^{-1}$; $\varepsilon_\eta = 0.6$ for $1000 \text{ cm}^{-1} < \eta < 2600 \text{ cm}^{-1}$; $\varepsilon_\eta = 0.7$ for $2600 \text{ cm}^{-1} < \eta < 4400 \text{ cm}^{-1}$; $\varepsilon_\eta = 0.8$ for $4400 \text{ cm}^{-1} < \eta < 6000 \text{ cm}^{-1}$; and $\varepsilon_\eta = 0.9$ for $6000 \text{ cm}^{-1} < \eta < 25\,000 \text{ cm}^{-1}$. Both walls were assumed to be identical, although the proposed methodology is not restricted to these scenarios. The spectral modeling of the problem is solved by applying the WBW model and the LBL solution to each one of the segments in which the spectrum was divided. The set of correlations of the WBW model for 4 gray gases in each one of the five spectral intervals, presented by Fonseca, 2022, was used. The segments in which the spectrum was divided are the same that were mentioned in the description of the emissivity profile of the surfaces. The results were obtained in terms of the radiative heat flux and radiative heat source and compared against the LBL solution, and they will be present in the next section.

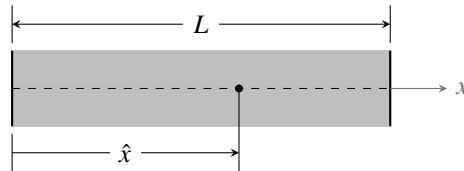


Figure 1. Schematic representation of the one-dimensional medium slab.

3. RESULTS AND DISCUSSION

In order to evaluate the accuracy of the proposed methodology regarding the LBL integration, three temperature profiles were tested, which are given by the following equations

$$T(\hat{x}) = 400 + 1400 \sin^2(\pi\hat{x}), \quad (19)$$

$$T(\hat{x}) = 400 + 1400 \sin^2(2\pi\hat{x}), \quad (20)$$

$$T(\hat{x}) = \begin{cases} 880 + 920 \sin^2(2\pi\hat{x}), & \text{if } \hat{x} \leq 0.25 \\ 400 + 1400 \left\{ 1 - \sin^{3/2} \left[\frac{2\pi}{3}(\hat{x} - 0.25) \right] \right\}, & \text{if } \hat{x} > 0.25 \end{cases}, \quad (21)$$

where $\hat{x} = x/L$ is the dimensionless distance from the left wall. Eq. (19) presents a profile with simple symmetry in relation to the x -axis, with both walls at 400 K, average temperature of 1100 K and maximum temperature of 1800 K. Eq. (20) is a doubly symmetrical profile in relation to the x -axis, with the walls and the average and maximum temperatures analogous to the previous profile. Eq. (21) represents a profile without symmetry, with average and maximum temperatures of 1100 K and 1800 K, respectively, and the left wall at 880 K and the right wall at 400 K. Fig. 2(a) shows the behaviors of these temperatures profiles.

In addition, three mole fraction profiles were also evaluated, according to the equations below

$$Y_c(\hat{x}) = 0.1 \sin^2(\pi\hat{x}), \quad (22)$$

$$Y_c(\hat{x}) = 0.1 \sin^2(2\pi\hat{x}), \quad (23)$$

$$Y_c(\hat{x}) = \begin{cases} 0.1 \sin^2(2\pi\hat{x}), & \text{if } \hat{x} \leq 0.25 \\ 0.1 \left\{ 1 - \sin^{3/2}[2\pi/3(\hat{x} - 0.25)] \right\}, & \text{if } \hat{x} > 0.25 \end{cases}, \quad (24)$$

in which Y_c is the mole fraction profile of CO_2 . In Eq. (22), the CO_2 mole fraction profile has simple symmetry in relation to the x -axis, with a peak of 0.1 in the middle of the domain and an average value of mole fraction equal to 0.05. Eq. (23) presents a profile with double symmetry in relation to the x -axis, with two peaks of 0.1 in $\hat{x} = 0.25$ and $\hat{x} = 0.75$, and an average fraction of $\overline{Y_c} = 0.05$. Finally, Eq. (24) does not present symmetry in relation to the x -axis, although the average and maximum values of Y_c are 0.05 and 0.1, respectively, as in both previous profiles. In Fig. 2(b) is presented these mole fraction profiles. In all the cases, the mole fraction of water vapor Y_w is twice that of carbon dioxide (i.e., $Y_w = 2Y_c$), so that the ratio between the partial pressures of these species is kept constant at $p_w/p_c = 2$.

In order to describe the behaviors of T and Y_c along the domain and to calculate the radiative heat flux and radiative heat source, the temperature and CO_2 mole fraction profiles were merged in this section. The combinations were created based on whether or not there is symmetry about the x -axis. So, Eqs. (19) and (22) together are referred to as Profile 1, Eqs. (20) and (23) are referred to as Profile 2, while Eqs. (21) and (24) together are referred to as Profile 3.

The accuracy of the proposed methodology was tested against the LBL solution through calculations of percentage deviations. In this framework, a normalized percentage deviation was defined as

$$\Delta\phi = \frac{|\phi_{\text{LBL}} - \phi_{\text{WBW}}|}{\max(|\phi_{\text{LBL}}|)}, \quad (25)$$

where ϕ is either the radiative heat flux, q_r , or the radiative heat source, S_r , the subscripts “LBL” and “WBW” represent the LBL and WBW solutions, respectively, and the term $\max(|\phi_{\text{LBL}}|)$ is the maximum absolute value of ϕ .

To assess the accuracy of the proposed method regarding the LBL solution, a set of test cases was analyzed. The temperature and mole fraction profiles are given by Eqs. (19)–(24); the mole fraction of H_2O is twice that of CO_2 ($p_w/p_c = 2$) and the total pressure is 1 atm. Eqs. (9) and (17) are used to calculate the radiative heat flux for the LBL solution and the WBW model, respectively; for the radiative heat source, Eqs. (10) and (18) are used, respectively. The radiation spectrum is divided into five regions and to each spectral interval is assigned 4 gray gases via WBW model.

Fig. 3 presents the radiative heat flux and radiative heat source for Profile 1 (which is formed by the combination of Eq. (19) for the temperature profile and Eq. (22) for the CO_2 mole fraction profile). This figure shows the solutions with the LBL method and the WBW model assuming that the plates that bound the participating medium are non-gray, in addition to the approach with the WBW model proposed in Fonseca *et al.*, 2021a, but with black walls (curves in the aforementioned figure identified as “LBL”, “WBW non-gray” and “WBW black”, respectively). The normalized percentage deviations of the tested approaches in relation to LBL integration are shown in Table 1. By this table, one can observe a good agreement between the non-gray approaches, since the results obtained with the WBW model presented a maximum deviation regarding the reference solution of 6.1 % for q_r and 4.47 % for S_r . In the case in which the walls of the domain are wrongly assumed to be black, when they should be treated as non-gray, the deviations with the WBW model can reach 16.9 % and 8 % for the radiative heat flux and radiative heat source, respectively.

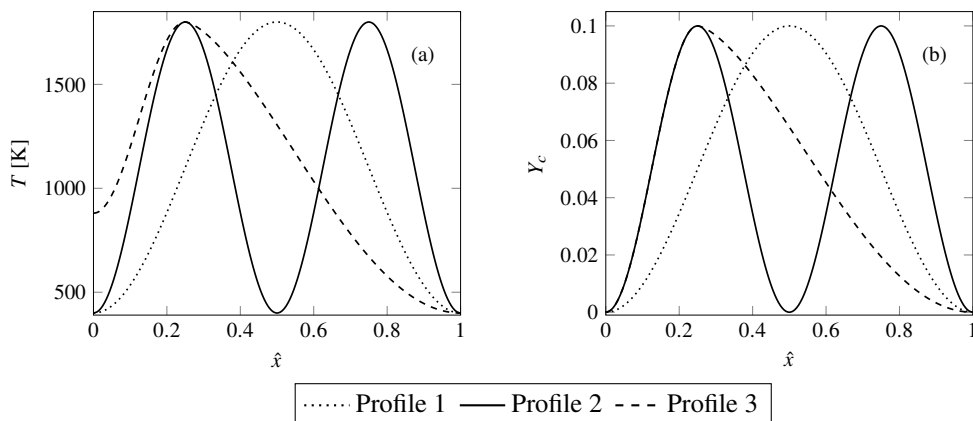


Figure 2. Profiles under study in this paper: (a) temperature profile; (b) CO_2 mole fraction profile.

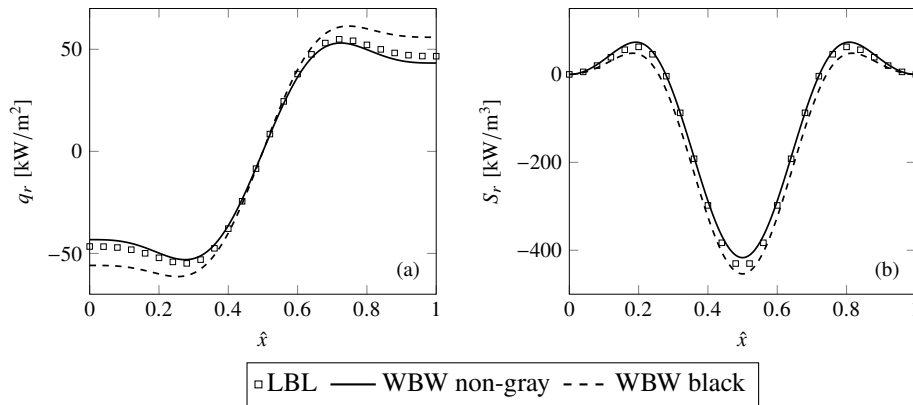


Figure 3. Radiative heat transfer for Profile 1: (a) radiative heat flux; (b) radiative heat source.

In Fig. 4, the radiative heat flux and radiative heat source for Profile 2 (formed by joining Eq. (20) for the temperature profile and Eq. (23) for the mole fraction profile of carbon dioxide) are shown. Analogously to the previous case, this figure presents the curves that represent the solutions for non-gray walls, obtained through the LBL and WBW methods, and the approach for black boundaries, also determined with the WBW model. According to the figure and Table 1, a satisfactory match between the approaches that describe the behavior of the solutions with non-gray surfaces was verified. For the radiative heat flux, the maximum error of the “WBW non-gray” approach in relation to the LBL integration was 6.68 %, and, for the radiative heat source, the maximum deviation was 5.95 %. Comparing the “LBL non-gray” solution and the approach with black walls, the maximum deviations for q_r and S_r were 18.93 % and 8.94 %, respectively.

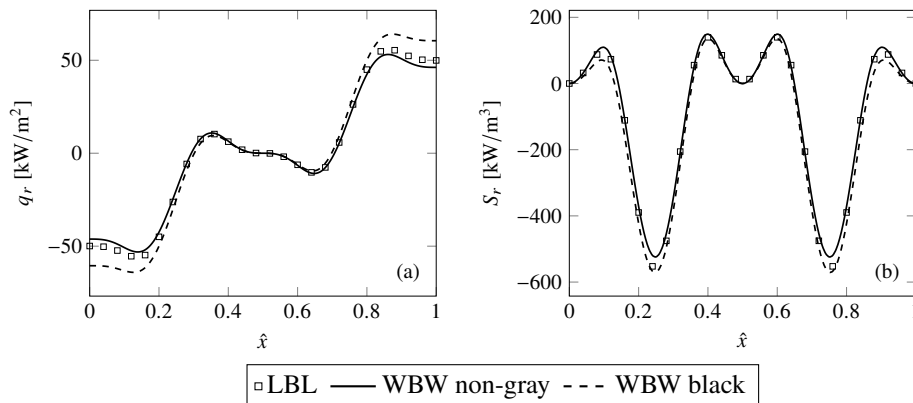


Figure 4. Radiative heat transfer for Profile 2: (a) radiative heat flux; (b) radiative heat source.

Finally, Fig. 5 depicts the behaviors of the radiative heat flux and radiative heat source for Profile 3 (Eq. (21) for the temperature profile and Eq. (24) for the mole fraction profile of carbon dioxide). By this figure and Table 1, it is noticed a greater discrepancy between the solutions for non-gray boundaries compared to the previous test cases, mainly with regard to the radiative heat flux, since the maximum error found was 8.13 %; for S_r , the maximum deviation in relation to the LBL method was close to that found with Profile 1, with a value of 4.56 %. When mistakenly treating the surfaces as black and when using the WBW model also to solve the spectral integration of the problem, the errors in relation to the reference solution reached 26 %, in the case of the radiative heat flux, and almost 10 %, for the radiative heat source.

In general, the application of the WBW model to the solution of non-gray surfaces presented a good performance when

Table 1. Maximum and average normalized deviations between the LBL integration and the different approaches of the WBW model.

Profile	LBL non-gray × WBW non-gray [%]				LBL non-gray × WBW black [%]			
	$(\Delta q_r)_{\max}$	$(\Delta q_r)_{\text{avg}}$	$(\Delta S_r)_{\max}$	$(\Delta S_r)_{\text{avg}}$	$(\Delta q_r)_{\max}$	$(\Delta q_r)_{\text{avg}}$	$(\Delta S_r)_{\max}$	$(\Delta S_r)_{\text{avg}}$
1	6.10	3.92	4.47	1.53	16.90	10.67	8.03	4.21
2	6.68	2.90	5.95	1.65	18.93	8.24	8.94	3.77
3	8.13	4.25	4.56	1.17	26.08	16.82	9.94	3.56

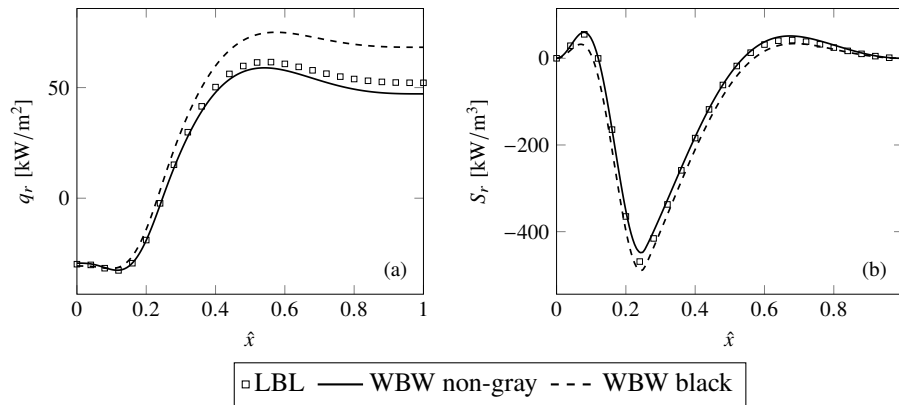


Figure 5. Radiative heat transfer for Profile 3: (a) radiative heat flux; (b) radiative heat source.

compared with the LBL method, since the maximum errors obtained were between 6 % and 8 % for the cases tested in the present study. According to the literature, when a wide-band model is adopted, which is the case of the WBW model applied in this paper, the accuracy even with black surfaces is unsatisfactory, since errors of 30 % are typically found (Modest, 2013). Based on this fact, the proposed methodology proved to be a great alternative, because even with non-gray surfaces it presented much better results than those reported in the literature. In future studies, it is initially planned to optimize the number of gray gases in each band in which the spectrum was divided according to the importance of each region for the calculation of the thermal radiation. Moreover, another perspective of study is to find other ways to synchronize the spectral intervals of the WBW model with the bands of the emissivity profile of the non-gray surfaces.

4. CONCLUSIONS

This paper presented a methodology for the application of the WBW model, which is a wide-band model based on the WSGG, for the calculation of the radiative heat transfer of a participating medium confined by non-gray walls. The methodology consists of assuming that the spectral intervals in which the radiation spectral was divided are coincident with the regions that represent the profile distribution of the spectral emissivity of the non-gray surfaces. A small set of test cases described by a non-isothermal and non-homogeneous mixture of water vapor and carbon dioxide was studied and the accuracy of the proposed methodology was evaluated against the LBL integration. The reference solution was also compared with the WBW model applied to black boundaries, in order to measure the discrepancies in assuming black surfaces that are actually non-gray. The results showed that the formulation presented in this paper leads to smaller deviations regarding the LBL solution than those found in the literature with the usage of band models. For future works, new ways of combining the bands of the WBW model with those of the emissivity profile of the boundaries will be investigated, as well as the inclusion of soot and other participating species.

5. ACKNOWLEDGEMENTS

Author FHRF thanks CNPq (Conselho Nacional de Desenvolvimento Tecnológico e Científico) for the research grant 302686/2017-7.

6. REFERENCES

- Bordbar, H., Coelho, F.R., Fraga, G.C., França, F.H. and Hostikka, S., 2021. "Pressure-dependent weighted-sum-of-gray-gases models for heterogeneous CO₂-H₂O mixtures at sub- and super-atmospheric pressure". *International Journal of Heat and Mass Transfer*, Vol. 173, p. 121207.
- Bordbar, H., Maximov, A. and Hyppänen, T., 2019. "Improved banded method for spectral thermal radiation in participating media with spectrally dependent wall emittance". *Applied Energy*, Vol. 235, pp. 1090–1105.
- Cassol, F., Brittes, R., França, F.H. and Ezekoye, O.A., 2014. "Application of the weighted-sum-of-gray-gases model for media composed of arbitrary concentrations of H₂O, CO₂ and soot". *International Journal of Heat and Mass Transfer*, Vol. 79, pp. 796–806.
- Coelho, F.R. and França, F.H., 2018. "WSGG correlations based on HITEMP2010 for gas mixtures of H₂O and CO₂ in high total pressure conditions". *International Journal of Heat and Mass Transfer*, Vol. 127, pp. 105–114.
- Denison, M.K. and Webb, B.W., 1994. "k-distributions and weighted-sum-of-gray-gases—a hybrid model". *Heat Transfer*, Vol. 2, pp. 19–24.
- Denison, M.K. and Webb, B.W., 1993. "A spectral line-based weighted-sum-of-gray-gases model for arbitrary RTE solvers". *Journal of Heat Transfer*, Vol. 115, No. 4, pp. 1004–1012.

- Dorigon, L.J., Duciak, G., Brittes, R., Cassol, F., Galarça, M. and França, F.H.R., 2013. “WSGG correlations based on HITEMP2010 for computation of thermal radiation in non-isothermal, non-homogeneous H_2O/CO_2 mixtures”. *International Journal of Heat and Mass Transfer*, Vol. 64, pp. 863–873.
- Fonseca, R.J.C., 2022. “A wide-band formulation based on the weighted-sum-of-gray-gases model for participating media with soot”. Doctoral thesis, Programa de Pós-graduação em Engenharia Mecânica, Universidade Federal do Rio Grande do Sul.
- Fonseca, R.J.C., Fraga, G.C., Coelho, F.R. and França, F.H.R., 2021a. “A wide-band formulation for the weighted-sum-of-gray-gases model applied to non-isothermal participating media”. In *Proceedings of the 26th International Congress of Mechanical Engineering*. ABCM.
- Fonseca, R.J.C., Fraga, G.C., da Silva, R.B. and França, F.H.R., 2018. “Application of the WSGG model to solve the radiative transfer in gaseous systems with nongray boundaries”. *Journal of Heat Transfer*, Vol. 140, No. 5, p. 052701.
- Fonseca, R.J.C., Fraga, G.C. and França, F.H.R., 2021b. “Grouping the wall spectral bands for an effective computation of the radiative transfer in participating media bounded by non-gray walls”. *International Communications in Heat and Mass Transfer*, Vol. 120, p. 105052.
- Gordon, I.E., Rothman, L.S., Hargreaves, R.J., Hashemi, R., Karlovets, E.V., Skinner, F.M., Conway, E.K., Hill, C., Kochanov, R.V., Tan, Y., Wcisło, P., Finenko, A.A., Nelson, K., Bernath, P.F., Birk, M., Boudon, V., Campargue, A., Chance, K.V., Coustenis, A., Drouin, B.J., Flaud, J., Gamache, R.R., Hodges, J.T., Jacquemart, D., Mlawer, E.J., Nikitin, A.V., Perevalov, V.I., Rotger, M., Tennyson, J., Toon, G.C., Tran, H., Tyuterev, V.G., Adkins, E.M., Baker, A., Barbe, A., Canè, E., Császár, A.G., Dudaryonok, A., Egorov, O., Fleisher, A.J., Fleurbaey, H., Foltynowicz, A., Furtenbacher, T., Harrison, J.J., Hartmann, J., Horneman, V., Huang, X., Karman, T., Karns, J., Kassi, S., Kleiner, I., Kofman, V., Kwabia-Tchana, F., Lavrentieva, N.N., Lee, T.J., Long, D.A., Lukashevskaya, A.A., Lyulin, O.M., Makhnev, V.Y., Matt, W., Massie, S.T., Melosso, M., Mikhailenko, S.N., Mondelain, D., Müller, H.S.P., Naumenko, O.V., Perrin, A., Polyansky, O.L., Raddaoui, E., Raston, P.L., Reed, Z.D., Rey, M., Richard, C., Tóbiás, R., Sadiek, I., Schwenke, D.W., Starikova, E., Sung, K., Tamassia, F., Tashkun, S.A., Auwera, J.V., Vasilenko, I.A., Vigasin, A.A., Villanueva, G.L., Vispoel, B., Wagner, G., Yachmenev, A. and Yurchenko, S.N., 2021. “The HITRAN2020 molecular spectroscopic database”. *Journal of Quantitative Spectroscopy and Radiative Transfer*, p. 107949.
- He, Z., Dong, C., Liang, D. and Mao, J., 2021. “A weighted-sum-of-gray soot-fractal-aggregates model for nongray heat radiation in the high temperature gas-soot mixture”. *Journal of Quantitative Spectroscopy and Radiative Transfer*, Vol. 260, p. 107431.
- Hottel, H.C. and Sarofim, A.F., 1967. *Radiative Transfer*. McGraw-Hill.
- Howell, J.R., Mengüç, M.P. and Siegel, R., 2016. *Thermal Radiation Heat Transfer*. CRC press, 6th edition.
- Lathrop, K.D. and Carlson, B.G., 1964. “Discrete ordinates angular quadrature of the neutron transport equation”.
- Liu, Y., Liu, G., Hu, H. and Kong, B., 2019. “A wavenumber subinterval grouping strategy compatible with non-gray metal wall boundaries used in multi-scale multi-group full spectrum k -distribution gas radiation model”. *Applied Thermal Engineering*, Vol. 162, p. 114216.
- Modest, M.F., 2013. *Radiative Heat Transfer*. Academic Press.
- Modest, M.F. and Haworth, D.C., 2016. *Radiative Heat Transfer in Turbulent Combustion Systems: Theory and Applications*. Springer.
- Modest, M.F. and Zhang, H., 2000. “The full-spectrum correlated- k distribution and its relationship to the weighted-sum-of-gray-gases method”. In *Proceedings of IMECE2000*.
- Rothman, L., Gordon, I., Barber, R., Dothe, H., Gamache, R., Goldman, A., Perevalov, V., Tashkun, S. and Tennyson, J., 2010. “HITEMP, the high-temperature molecular spectroscopic database”. *Journal of Quantitative Spectroscopy and Radiative Transfer*, Vol. 111, No. 15, pp. 2139–2150.
- Selhorst, A., Fraga, G., Coelho, F., Bordbar, H. and França, F., 2022. “A compact WSGG formulation to account for inhomogeneity of H_2O-CO_2 mixture in combustion systems”. *Journal of Heat Transfer*.
- Silva, R.M., Fraga, G.C. and França, F.H.R., 2021. “Improvement of the efficiency of the superposition method applied to the WSGG model to compute radiative transfer in gaseous mixtures”. *International Journal of Heat and Mass Transfer*, Vol. 179, p. 121662.
- Solovjov, V.P., Lemonnier, D. and Webb, B.W., 2013. “Efficient cumulative wavenumber model of radiative transfer in gaseous media bounded by non-gray walls”. *Journal of Quantitative Spectroscopy and Radiative Transfer*, Vol. 128, pp. 2–9.
- Solovjov, V.P. and Webb, B.W., 2002. “A local-spectrum correlated model for radiative transfer in non-uniform gas media”. *Journal of Quantitative Spectroscopy and Radiative Transfer*, Vol. 73, No. 2-5, pp. 361–373.
- Taine, J., 1983. “A line-by-line calculation of low-resolution radiative properties of CO_2-CO -transparent nonisothermal gases mixtures up to 3000 K”. *Journal of Quantitative Spectroscopy and Radiative Transfer*, Vol. 30, No. 4, pp. 371–379.
- Wang, B. and Xuan, Y., 2019. “An improved WSGG model for exhaust gases of aero engines within broader ranges of temperature and pressure variations”. *International Journal of Heat and Mass Transfer*, Vol. 136, pp. 1299–1310.

7. RESPONSIBILITY NOTICE

The authors are solely responsible for the printed material included in this paper.